CALCULATED HYDROXYL $A^2\Sigma \rightarrow X^2\Pi$ (() ,0) RAND EM I SS ION RATE FACTORS A} 'I' I.] CABLE 'T'[) ATMOSPHER I C S PECTROSCOPY

K. P. Cageao,† Y. 1,. Ha,‡ Y. Jiang,‖ M. F. Morgan,¶

Y. L. Yung,‖ and S . P. Sander†

I.let Propulsion Labora tory , Cal ifornia Inst i tute of Technology, Pasadena, California 91109,

‡ Department of Chemical Engi neeri ng, University of California, Berke 1 ey , California 94720,

‖Division o f Geological and Planetary Sciences, California Institute of Technology, Pasadena, California 91125, and

¶Applied Physics Laboratory, Johns Hopkins University, Johns Hopkins Road, Laurel , Maryland 20723

Abs trac t -- A calculat ion of the $A^2\Sigma \rightarrow X^2\Pi$ (0,()) band emission rate factors and 1 ine center absorpt ion cr oss sect ions of OH appl icable to its measurement using solar resonant f luorescence in the terrestrial atmosphere is presented in this paper. The most accurate available line parameters have been used. Special consideration has been given to the solar input flux because of its highly structured Fraunhofer spectrum. The calculation for the OH atmospheric emission rate factor in the solar resonant fluorescent case is described in detail with example s and intermediate results. Resul ts of this calculat ion of OH emission rate factors for individual rotational lines are, on average, 30% lower than the values obtained in an earlier work.

1 NTRODUCTI ON

The free radical hydroxyl (OH) is a key species in the closelycoupled chemist ry of odd ni t rogen, chlorine and oxy gen in the st ratosphere andlower mesosphere . In the st ratosphere OH part icipa tes in catalytic cycles with odd ni t rogen and odd chl orine whi ch affect theconcentration of ozone . I II the mesosphere OH and the odd hydrogen fami ly domi nat e the cat alyt ic photochemist ry and the dest ruct ion of ozone. The principal source of hydroxy] i n the upper at mosphere is the react ion between water vapor and $O(^1D)$. Above 60km di rect photol ysis of water vapor, derived f rom the oxi dat i on of CH_4 which is transported from the troposphere , becomes impel-t ar]t.. The primary si nk f'or OH in the st rat osphere and mesosphere is through i ts reaction wi th HO_2 .

Despi te the import ance of hydroxyl to the understanding of upper atmospheric chemi st t-y, onl y a few measurements of OH concent rat ion in the upper atmosphere exis L. The di fficul ty in measuring this low abundance species stems from i t s ext reme reactivi ty and short chemical 1 i fetime . The exi st ing techniques for OH concent rat ion measurements include bal loon borne UV L. IDAR[1] and far- infrared spect.remet.ers , [2, 3] UV laser induced fluorescence,[4] and solar resonant. f luoresce nce . [5,6] Because of the large electronic cross section of OH in the near ultraviolet, the OH resonant fluorescence emission can be detected by spacecraft-borne remo te sensing spectrometers. 'l'his technique could be applied to global mapping and long-term monitoring of OH between 40 and 80 km. To permit the conversion of emitted OH band intensities to OH concentrations, precise knowledge of the spectroscopic paramete rs governing the fluorescent. emission is required. A thorough knowledge of the input solar irradiance required to electronically excite OH is also required as well as the transition probabilities for de-excitation and emission through a large number of vibrational -rotational pathways.

line strengths and solar resonant. fluorescence emission rate factors have been calculated for hydroxyl rotational lines in cart-h's upper atmosphere.' However, explicit steps and intermediate results necessary for the calculation have not. been presented. The details of our calculation

are presented here including the considerations involving the selection of a solal" irradiance spectx-a which strongly influences the resultant values of OH emission rate factors.

ANALYSIS

The emission rate fact_ or, or Chamberlain g-factor, relates the specific intensity, I, of a part. icul at- vibrational-rotational transition to the observed column abundance of the emitting molecule:[8]

$$4\pi I = g(v,v')\ q(z) \qquad (1)$$

where 4711 is the emitted flux in Rayleighs[8] in 4π steradian, $\eta(z)$ is the column abundance (molecules·cm^{-2}) along the observed path, and $g(v,v')$ is the emission rate or g-factor (photons·sec^{-1}). For a single vibrational band the g-factor can be expressed as:[9]

$$g(v,v') = \frac{\pi e^2}{m c^2}\ \pi F\ \lambda^2(v,v')\ f(v,v')\ \frac{A(v,v')}{\sum_{v} A(v,v')} \qquad (2)$$

where the un-primed v is the initial vibrational level of the resonant pumping and v′ is the first excited level ($A^2\Sigma$ electronic state, v′=0 for 0}[) to which the molecules are pumped, πF is the spectral disk integrated solar irradiance, e is the elect.ron charge (in esu), m is the electron mass (in grams), c is the speed of light., λ is the transition wavelength, $f(v,v')$ the vibrational transition band oscillator strength, and $A(v,v')/\sum_{v} A(v,v')$ the Einstein coefficient branching ratio for a particular vibrational state.

For individual rotational lines within the hydroxyl vibrational band the g-factor equation must be expanded to include:

$$g(v',v'',J',J'',T) = \frac{\pi e^2}{mc^2}\sum_{v}\sum_{J} \pi F[\lambda^2(v,v',J,J')]f(v,v',J,J') \times N(v,v',J,J',T)\Big\} \frac{A(v',v'',J',J'')}{\sum_{v''}\sum_{J''} A(v',v'',J',J'')} \qquad (3)$$

where v′ and J′ (the rotational level) are Lhe state to which the molecules are pumped, and v″ and J″ are the lower state ($X^2\Pi$ ground electronic state for 01{) to which the molecules relax. πF is determined at the pumping wavelength, $\lambda(v,v',J,J')$, $N(v,v',J,J',T)$ is the rotational population of the initial level at. equilibrium temperature T. $f(v,v',J,J')$ is the rotational

line oscillator strength given by:

$$f(v, v', J, J') = f(v, v')\, \lambda^2(v, v', J, J')\, \frac{S(J', .1'')}{4(2J''+1)} \qquad (4)$$

where S(J ' ,. 1") is the rotational line strength[10] for the transition. In Eq (4), J" is equivalent to J since the absorption (pumped) transition, v,J -> v' ,.1', used to define oscillator strength is the same as the emission transition, v', J'-> v" J".

The OH ground electronic configuration is $X^2 11$. The $^2\Pi$ state is split fnto two states, the $^2\Pi_{1/2}$ and the $^2\Pi_{3/2}$ states. The $^2\Pi$ states are each split by the magnetic interaction between the angular momentum of molecular rotation and the orbital angular moment urn (f_1 and f_2 states). These Λ-doubled levels are in turn split by the coupling of the molecular magnetic moment, M, with the spin of the hydrogen nucleus, but the difference in energy of this hyperfine structure is small (less than 0.01 cm^{-1}) and has been neglected here. For the first excited state of 01[, $^2\Sigma$, the rotation vector, N, takes on values J=N± 1/? (F_1 and F_2 states, respectively). Thus for each N sLa Le there are at least Lwo J levels.

For OH rotational transitions between the above two electronic states, dipole select-ion rules dictate that ΔJ= 0,±1 and a parity (+ or -) change occurs between the levels. Transitions ΔJ= -1, 0, and +1, are allowed and designated i', Q, and R, respectively. Transitions are subscripted to indicate which of the split states the Transition originates from and which it. Germinates in. A subscript 1 indicates N=J+ 1/2 (F_1 for $A^2\Sigma$ and f_1 for $X^2 11$ rotational levels) and subscript 2 indicates N= J-1/2 (F_2 for $^2\Sigma$ and f_2 for 211). The first subscript of P, Q, or R gives the upper ($^2\Sigma$) state and the second the lower ($^2\Pi$) state. For the case where the upper and lower states are F_1 and f_1 or F_2 and f_2 (main branches), only one subscript is used. A leading superscript for changes in N is included: O, P, Q, R, S (ΔN= -2,-1,0,+1,+2) when the. transition arises from a change in *electron* spin and ΔJ≠ΔN (satellite branches). Thus, $^QR_{12}(4)$ is a transition where ΔN=0, ΔJ=1, with upper state F_1 and lower state f_2 originate from Or emit. to lower rotational level N"=4. Altogether there are 1? possible transitions, 6 main branches: P_1, P_2, Q_1, Q_2, R_1, R_2, and 6 satellite branches: $^0P_{12}$,

$^{P}Q_{12}$, $^{Q}R_{12}$, $^{Q}P_{21}$, $^{R}Q_{21}$, $^{S}R_{21}$ for a given N level (see Fig. 1).

Precise hydroxyl rotational line positions are necessary for OH emission rate factor calculation because of the highly structured input solar Fraunhofer spectrum. To derive the term values, energies, and calculated line positions of the hydroxyl ultraviolet emissions two techniques have been used, direct diagonalization[11,12] and perturbation analysis,[13] to derive the Hamiltonian for the hydroxyl wave function. The eigenvalues of the derived Hamiltonian are the term values of the hydroxyl states. Goldman and Gillis[14] (hereafter, GG) used the unique perturber approximation, a diagonalized 3 x 3 Kronig transformed Hamiltonian matrix and a set of Hamiltonian constants derived by Destombes[15] to arrive at the term values for the OH $^{2}\Sigma_{1/2}$, $^{2}\Pi_{1/2}$, and $^{2}\Pi_{3/2}$ states. Term value wavenumbers are referenced to the $^{2}\Pi_{3/2}$ f_{1c} N"=1 state and are listed in Tables 1a and 1b by state. Line positions resulting from these term values have a stated accuracy of $0.1 cm^{-1}$. Recently measured OH line positions[16] show the GG calculated positions are within $\pm 0.08 cm^{-1}$ for all rotational lines N"≤15. The GG line positions differ from the measured line positions by less than the doppler width of the atmospheric OH lines ($0.09\ cm^{-1}$).

Chidsey and Crosley[17] give the Einstein transition probability of a rotational line transition (Eq. (3)) as:

$$A(v', v'', J', J'') = \frac{64\pi^4\nu^3}{3h}\, p(v', v'', J', J'')\, \frac{S(J', J'')}{(2J'+1)} \qquad (5)$$

where h is Plank's constant, ν is the wave number of the rotational line, $p(v', v'', J', J'')$ is the band strength, and $S(J', J'')$ is the rotational line strength normalized such that $\sum_{J''} S(J', J'') = 2J'+1$. Single primed quantities represent $^{2}\Sigma$ level v or J, and double primes are $^{2}\Pi$ level quantities. Chidsey and Crosley[18] have tabulated relative values of the Einstein coefficients normalized to the probability of the $P_1(1)$ transition Using values of $S(J', J'')$. Placing these Einstein coefficients on an absolute reference scale, the measured lifetimes [$\tau(v'J')$] of a selected $^{2}\Sigma$ states is:

$$\tau(v'J') = [\sum_{v'', J''} A(v', v'', J', J'')]^{-1} \qquad (6)$$

Chidsey and Crosley[17] give values for the ratio of Einstein coefficients for a number of the OH vibrational bands. They find A(f), 1)/(A0, 0)= 3. 7x10-3 [the form of the notation is A(v', v")] and A(0, 2)/A(0, 0)= 9 .7x10-> indicating that transitions to vibrational levels other than v"= 0 are negligible. Thus, the sum of' calculated τ(v'J') for v"=0 alone compared with the measured values of τ(v'J') gives the factor necessary to obtain absolute A(v' ,v", J' ,J")

The measured lifetime for the rotationless (N'=0) OH molecule, τ(v'=0,J'=1/2), is difficult to obtain experimentally because of uncertainties in the electronic quenching rate. Lifetime measurements must be made under conditions of very low pressure (less than 1mtorr).[19] The average of recently obtained values for the OH lifetime results in: τ(0,½)= 690±70ns.[19-24] The (0,0) band oscillator strength, f(0,0) is related to τ(0,½) by:[25]

$$f(0,0) = \frac{m\,c}{8\pi^2 e^2 \nu^2} \frac{1}{\tau(0,\tfrac{1}{2})} \frac{g_n}{g_m} \qquad (7)$$

where m is the mass of an electron, c is the speed of light, e is the electron charge, ν is the wavenumber of the band origin [for OH (0,0) 32404.407cm-1 or 3086Å], and where g_n and g_m are the degeneracies of the upper and lower states, respectively. With τ(0,½)= 690±70ns Eq. (7) gives f(0,0)= 1.04±0.1x10^{-3}. The 10% uncertainty in the lifetime measurement leads directly to a 10% uncertainty in the hydroxyl line g-factors and 10% uncertainty in the retrieved hydroxyl concentrations using the resonant fluorescence method. Further validation of the hydroxyl lifetime measurements is required for greater accuracy in the determination of the OH rotational line emission rate factors.

GG calculate the rotational line strengths based on a method described by Hougen[26] and Whiting and Nicholls[27] to take into account the perturbations to the electronic dipole moment due to centrifugal and higher order distortions and the interactions between the $A^2\Sigma$ and $X^2\Pi$ states.[14] GG normalize their line strengths using:

$$\sum_{\Sigma, J'} S(J,'J") = 4(2J"+1) \qquad (8)$$

where the subscript Σ indicates the sum is to include both spin states of the $X^2\Pi$ configuration. Thus, when using the GG values of $S(J',J'')$, the normalization factor of 4 in the denominator of Eq. (4) may be omitted.

GG use their calculated values of line Strength, Chidsey and Crosley's[17] ro-vibrational transition probabilities, and equation (5) to calculate Einstein A coefficients. The Einstein coefficients arc adjusted by GG to obtain an absolute A value. by using German's[20] $\tau(0,\frac{1}{2})$= 68811S and Eq. (6). The result is listed in 'i'able 2. The average of recent measure merit-s of the OH lifetime [$\tau(0,\frac{1}{2})$= 690ns] suggest tha L the 1 ife time of the rotat ionless hydroxyl molecule may be s] ight ly longer. The absolute rotational line Einste in coefficients calculated by GG can be adjusted to the sl igh tly longer lifet ime values used in this work by multi plying the GG Einstein coeffic ients by the ratio of" the lifetimes (688ns/690ns)

I f the hydroxyl molecules i n the atmosphere are in thermal equilibrium, the rotational population distribut ion can be described by the Maxwell-Bol tzmann dist ribut ion law. For a normalized distribution, the rotational population is given by:[28]

$$N(v, v', J, J', T) = (2J+1)[\exp\{hcE(J)/(kT)\}]/Q(T) \qquad (9)$$

where h is Plank's constant, c is the speed of light, E(J) the energy (in cm^{-1}) of the $X^2\Pi$ J stat-e, k is the Bolt zmann constant, T is the equilibrium temperature (in kelvins), and Q(T) is the partition function.

The partition function, Q(T), has both vi brat ional, Q_v, and rotational, Q_r, part-s. If the partition function is separable, Q(1) is $Q_v \cdot Q_r$. The. harmonic oscillator approximation for the vi brat ional part ition functi on is:[29]

$$Q_v = (1 - \exp[hc\omega_e/(kT)])^{-1} \qquad (lo)$$

where ω_e is the first order vibrational constant equal to 3737.761 cm^{-1}.[29] Because of this large energy separation between vi brational levels, the value of Q_v is nearly unity at. middle atmospheric tempera tures. '1'bus, the OH molecules normally lie in the lowest vibrational st ate, v"= (), of the $X^2\Pi$ electronic state. 'he rotational part ition function is:

$$Q_r = \sum_{J'', \Sigma''} (2J''+1) \exp\left[hcE(J'', \Omega'')/(kT) \right] \quad (11)$$

where the summation is over both J" rotational levels and spin sub-states of $^2\Pi_{3/2}$ and $^2\Pi_{1/2}$. Table 3 lists the population distribution at 200, 240, and 300K. The transitions are listed in groups of three since they all arise from the same J", $^2\Pi_{\Sigma''}$, and lower state N value. The groups differ in the $^2\Sigma$ state F, J or N values to which they are pumped.

Selection of the input solar flux spectrum is crucial to an accurate rotational line g-factor determination for hydroxyl. The value of the emission rate factor is dependent on the solar input pumping to the $A^2\Sigma$ state. The near ultraviolet spectrum of the sun is highly structured with many deep Fraunhofer absorption features. A disk integrated solar spectrum with spectral resolution near the doppler width of the terrestrial hydroxyl lines ($0.09 cm^{-1}$ or 0.009A) is required for the g-factor calculation but no calibrated, absolute irradiance solar spectral with this resolution exist-s for the 3000 to 3200Å near-UV spectral region. The Kohl, Parkinson, and Kurucz[30] (hereafter, KPK) atlas is relatively high resolution (0.028A at 2537Å) but is not disk integrated and solar 1 imb darkening was not measured longward of 3060Å. Applying broad spectral bandpass analytical expressions for the limb darkening[31] distorted the Fraunhofer line peak intensities and were rejected as incompatible with lower resolution data sets.[32,33,34] The data set. from the Solar Maximum Mission spacecraft Ultraviolet Spectrometer (UVSP)[35] has a resolution of 0.04Å bet.wcen 1750 and 3600Å but grating drive instabilities, an incomplete spectral data set, and the lack of an absolute irradiance scale, make this data set difficult. to use.[36] A high resolution exo-atmospheric spectrum for the near ultraviolet- must be constructed from lower resolution spacecraft data and adjusted high resolution ground-based spectra.

Absolute, disk integrated, near-UV solar irradiance spectra have been obtained from space at spectral resolutions of 3.2A by the Upper Atmosphere Research Satellite (UARS) Solar-Stellar Irradiance Comparison Experiment (SOLSTICE).[37,38] With extensive pre- and in-flight calibrations, SOLSTICE is designed to accurately measure the full disk solar spectral irradiance

between 1150 and 4200Å to a 2σ absolute accuracy of 10%. A recent intercomparison[39] shows that irradiances measured by several instruments including SOLSTICE above 200nm agree to better than 15%. The UARS SOLSTICE data set was chosen as the photometric standard to be used to adjust a high resolution ground based solar spectrum to exo-atmospheric values.

A high resolution ground based solar spectrum with excellent signal-to-noise and wavelength coverage has been compiled by the National Solar Observatory (NSO Atlas No. 1)[40] using the Kitt Peak McMath-Pierce Solar Telescope's Fourier Transform Spectrometer. The spectrum covers the wavelengths 2960 to 13000Å at a resolving power of 348,000 in the ultraviolet (0.0086Å at 3000). This resolution exceeds the doppler width of the terrestrial OH lines. Adjustment factors in bands of 20Å are presented in the atlas to obtain exo-atmospheric flux by comparing the observed "pseudo-residual fluxes" with several spectral data sets. These data sets include sounding rocket measurements,[31] SpaceLab 1 measurements,[42] and aircraft measurements[43] covering the range from 3000A to 3200Å. Figure 2a compares the NSO atlas adjusted solar irradiances with the SOLSTICE solar atlas for the spectral region 3000 to 3200Å. The SOLSTICE data is presented at the full instrument measured resolution of 3.2Å plotted every 0.7A and the high resolution NSO spectrum has been degraded to the SOLSTICE 3.2Å resolution using a simulated instrument triangular slit function with full width at half maximum equal to the SOLSTICE resolution. Figure 2b is a plot of the ratio of the SOLSTICE to NSO irradiance every 0.7A in 20Å spectral bands matching the pseudo-residual flux adjustment band used in the NSO atlas. In the spectral region 3000 to 3200Å, the spectra differ by up to 18% in these 20A bands. An 8th order polynomial has been fit to this difference and plotted in Fig. 2b. This fit to the SOLSTICE:NSO irradiance ratio has been applied to the NSO high resolution spectrum to adjust it to match the SOLSTICE irradiance values as shown in Fig. 2c. There is good agreement between the adjusted NSO and the SOLSTICE irradiances.

Applying the above analysis to the calculation of OH g-factors, incorporating GG OH rotational transition wavelengths, Einstein rotational transition probabilities, rotational line strengths, rotational population

distribution, the SOLSTICE adjusted NSO atlas high resolution solar flux values, and a band oscillator strength of 1.04×10^{3} results in the g-factors listed in Table 4 for all 12 of the OH branches up to and including rotational level N"=15. The list includes emission rate values at 200, 240 and 300 K. The uncertainty in this calculation, derived primarily from the ±10% uncertainty in the oscillator strength, an ±8% uncertainty in OH line center solar flux (the maximum line center absorption in the solar spectrum due to the ground based OH column in the NSO data), and an assumed ± 10% 2σ absolute irradiance uncertainty in the SOLSTICE derived solar spectral is ±28%.

The emission rate factors calculation in this work are on average 30% lower than the results published in an earlier work.[7] It is difficult to address the specific cause of this discrepancy since intermediate results were not presented in the earlier paper. The probable cause, however, is the adopted solar flux.

Table 5 is included as an aid to those wishing to modify or reproduce the g-factor calculation in this paper. The table lists the 10 strongest emission lines at. 240 K, as well as the OH absorption lines pumped to populate the $A^2\Sigma$ emitting level. For each of the absorption transitions, the wavelength, solar flux, Einstein coefficient, population, and rotational line strength are listed below the result-ant emission line transition, wavelength and emission rate factors at. 240K.

The sensitivity of the calculated emission rate factors to solar spectral doppler shifts in the cart.tl's reference frame were also investigated. These are dependent. on the earth's orbital position and the solar declination and hour angle at the observing site and are on the order of 0.1 cm-l. The percentage changes in the OH rotational line g-factors for the ten strongest lines at 240K are shown in Table 6 (along with the populating absorption line solar fluxes: see Table 5) for solar spectral wavelength shifts of $+0.1 cm^{-1}$ and $-0.1 cm^{-1}$ relative to the NSO atlas solar line positions. The effect of spectral wavelength shifts on these strong lines is as much as 14%. Weaker line g-factors changed up to 33%. Precise

corrections ["0 1" varying spectral doppler shifts due to earth orbits] eccentricity, solar declination and hour angle, as well as accurate solar atlas l'l"aLIIlllofct- 1 ine positions is imperative to deduce the OH abundances from observed emission intensities.

Conclusions

This paper has presented a calculation of the hydroxyl emission rate fact or-s applicable to the measurement of OH in the terrestrial atmosphere using solar resonant fluorescence spectroscopy. The most accurate available transition wavelengths, Einstein transition probabilities, band oscillator strength, rotational line strengths, and rotational level population (distributions have been used. Special consideration was given to the high resolution input solar spectrum because of the highly structured Fraunhofer spectrum in the near UV. The importance of an ac.curate solar spectrum and wavelength scale are underscored by a calculation herein indicating the hydroxyl emission rate factor can change as much as 14% for a shift in the solar spectrum wavelength scale of as little as $\pm 0.1 cm^{-1}$. The calculation for the OH atmospheric solar resonant fluorescent. case has been present.eci in detail in order to facilitate future calculations with refined line parameters and solar flux values.

AC KNOWLEDGEME NTS

The authors woul d 1 i ke to thank Xi aolei Zhu for his efforts in refining the program coding , Drs Wi 1 l i am Sharp and Randal 1 Frie dl for thei r support , he l pful comment s , and di scussi ons refining the scope of" this pape r, and Drs . Gary Rot tman and Robert Kurucz for i] luminat ing di scussions on the solar near ult raviolet spect t-a. Thi s work was supported by NASA Sounding Rocket. Fl ight Program grant NGR 23-00 S-36, NASA Gt-actuate Student Researcher's Grant. NGT- 50010, NASA grant NAGW - 2204, a Cal ifornia Ins titute of Technology Summer Undergraduate Researche r Fund grant and President ' s Fund grant, and a Je t Propulsion Labora tory Di rector' s Di scre tionary Fu ıd grant .

REFERENCES

1. W. S. Heaps and 'l'. J. McGee, *J. Geophys.Res.* 90, 7913 (1985) .

2. [). G. Johnson, K. W. Jucks, W. A. Traub, and K. V. Chance, *J. Geophys. Res.* **100**, 3091 (1995).

3. II. M. Pickett and [). B. Peterson, *J. Geophys. Res.* 98, 20507 (1993)

4. P. O. Wennberg, T. F. Hanisco, R. C. Cohen, R. M. Stimpfle, L. B. Lapson, anti J. G. Anderson, *J. Atmos. Sci* . 52, 3413 (1995) .

5. M. F. Morgan, D. G. Torr, and M. R. Torr, *Geophys.Res.Lett.*20,511 (1993).

6. D. Offermann and R. R. Conway, *EOS Trans.* 76, 337 (1995) .

7. J. A. Fennelly, D. G. l'err, and M. R. Torr, *J. Geophys. Res.* 94, 5183 (1989).

8. J, W. Chamberlain, *Physics of the Aurora anti Airglow*, Academic Press, New York (1965) .

9. J. B. Pearce, *J. Quant. Spect. Rad. Trans.* 9,]593 (1969).

10. R. F. M. Bennett, *Mon. Not. R. Astro. Sot.* 14"/, 35 (1970) .

11. R. L. Poynter anti R. A. Beaudet, *Phys.* Rev. *Lett.* 21, 305 (] 968) .

12. D. 1,. Cooper and L. Veseth, *J. Chem. Phys.* 74, 3961 (1981) .

13. G. c. Dousmanis, T. M. Sanders, Jr., and C. H. Townes,*Phys.Rev.*100, 1735 (1955).

14. A. Goldman and J. R. Gillis, J. *Quant. Spect. Rad. Trans. 25,* 111 *(1981).*

]s. J. Destombes, C. Marliere, and F. Rohart, *J. Molec. Spect.* **67**, *93, (1977).*

16. G. Stark, J. W. Brault, and M. C. Abrams, *J. OpticalSoc.Am.B***11**, *3 (1994)*

17. I. 1,. Chidsey and D. R. Crosley, *J. Quant. Spect. Rad. Trans.* 23, 18-1 (1980) .

18. 1. L. Chidsey and D. R. Crosley, Tables of Calculated Transition Probabilities for the A-X System of OH, *Tech. Rep. ARBRL-TR-02326*, Ballistic Research Laboratory, Aberdeen Proving Ground, ME). (1981).

19. I. S. McDermid and J. B. Landenslager, *J. Chem. Phys. 76, 1824* (1982) .

20. K. R. German, *J. Chem. Phys. 63,* 5252 *(]975)* .

21. J. H. Brophy, J. A. Silver, and J. I,. Kinsey, *Chem. Phys. Lett.* 28, *418 (1974).*

REFERENCES (continued)

22 J. Brzozowski, P. Erman, and M. Lyyra, *Phys. Scripta* **17**, 507 (1978).

23 W. L. Dimpfl anti J. L. Kinsey, *J. Quant. Spect. Rad. Trans.* **21**, 233 (1979).

24 C. C. Wang and C. M. Huang, *Phys.* Rev. A. 21, 1?35 (1980).

25 H. Okabe, *Photochemistry of Small Molecules*, J. Wiley & Sons Inc., New York (19-18).

26 J. T. Hougen, The Calculation of Rotational Energy Levels and Rotational Line Intensities in Diatomic Molecules, *NBS Monograph 115*, Us. Government Printing Office, Washington, D. C. (1970).

27 E. E. Whiting and R. W. Nicholls, *Astrophys. J. Supp.* **27**, 1 (19/4).

28 I. Kovacs, *Rotational Structure in the Spectra of Diatomic Molecules*, American Elsevier Pub. Co., New York (1969)

29. G. Herzberg, *Molecular Spectra and Molecular* Structure *I. Spectra of Diatomic* Molecules, Van Nostrand Reinhold co., New York (1950).

30. J. L. Kohl, W. 11. Parkinson, and R. L. Kurucz, *Center and Limb Solar Spectrum in High Resolution 225.2 nm* to *319.6 nm*, Havard Smithsonian Center for Astrophysics (1978).

31. O. K. Moe and E. F. Milone, *Astrophys. J.* 226, 301 (1978).

32. M. E. VanHoosier, J.-D. F. Bartoe, G. E. Brueckner, and D. K. Prinz, *Astrophys. Lett. & Comm. 27, 163* (1988a).

33. G. H. Mount and G. J. Rottman, *J. Geophys. Res.* **90**, 13031 (1985).

34. L. A. Hall, *J. Geophys. Res.* 86, 555 (1981).

35. B. E. Woodgate, et al., *Solar Physics* 65, 73 (1980).

36. R. L. Kurucz, personal communication (1992).

37. G. J. Rottman, T. N. Woods, and T. P. Sparn, *J. Geophys. Res.* 98, 10667 (1993).

38. T. N. Woods, G. J. Rottman, arid G. J. Ucker, *J. Geophys. Res.* 98, 10679 (1993).

39. T. N. Woods, et al., *J. Geophys. Res.* (accepted for pub. 1996)

40. R. L. Kurucz, I. Furenlid, J. Brault, and L. Testerman, *Solar Flux Atlas from 296 to 1300nm*, National Solar Observatory, Sunspot, New Mexico (1984).

41. A. L. Broadfoot, *Astrophys. J. 173, 681 (19"/?)*

42. D. Labs, H. Neckel, P.C. Simon, arid G. Thuillier, Solar *Physics* **107**, 203 (198-/).

REFERENCES (continued)

43. J. C. Arvesen, R. N. Griffin, Jr., and B. D. Pearson, Jr., *Appl. Opt.* 8, 2215 (1969).

FIGURE CAPTIONS

Figure	Caption
1	OH rotational transition manifold for $A^2\Sigma \rightarrow X^2\Pi$
2a	SOLSTICE solar spectrum (solid line) and NSO atlas spectrum (dashed line) at 3.2A resolution. Wavelengths at STP air and fluxes are in photons/cm^2/sec/A.
2b	Ratio of SOLSTICE to NSO flux every 0.7A (dotted line), in 20Å spectral bands (solid line), and an eighth order polynomial fit to the 20Å spectral band data (heavy solid line)
2c	SOLSTICE solar spectrum (solid line) compared with adjusted NSO solar spectrum (dashed line). Resolution for both spectra is 3.2Å

0}{ $^2\Pi_i$ - $^2\Sigma^+$ Band Rotational Transitions

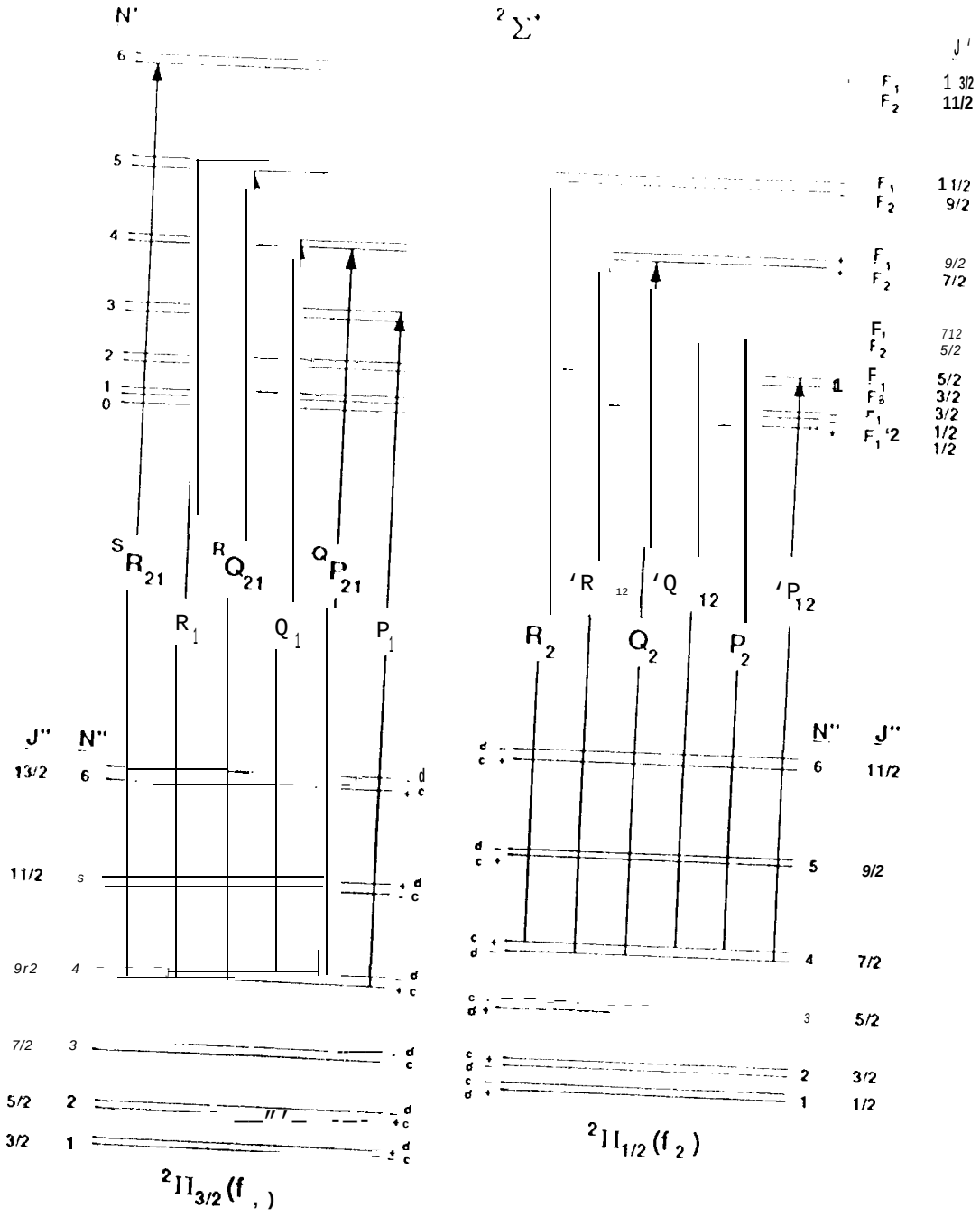

Fig. 1

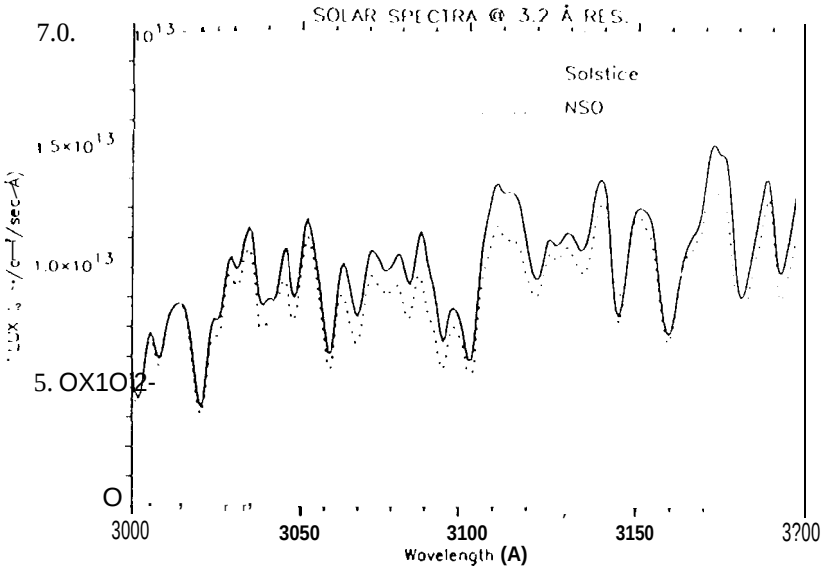

Fig. 2a

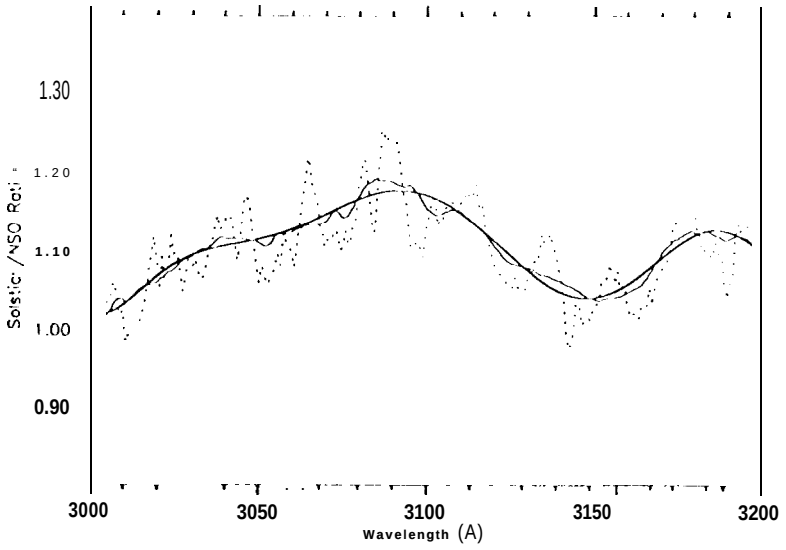

Fig. 2b

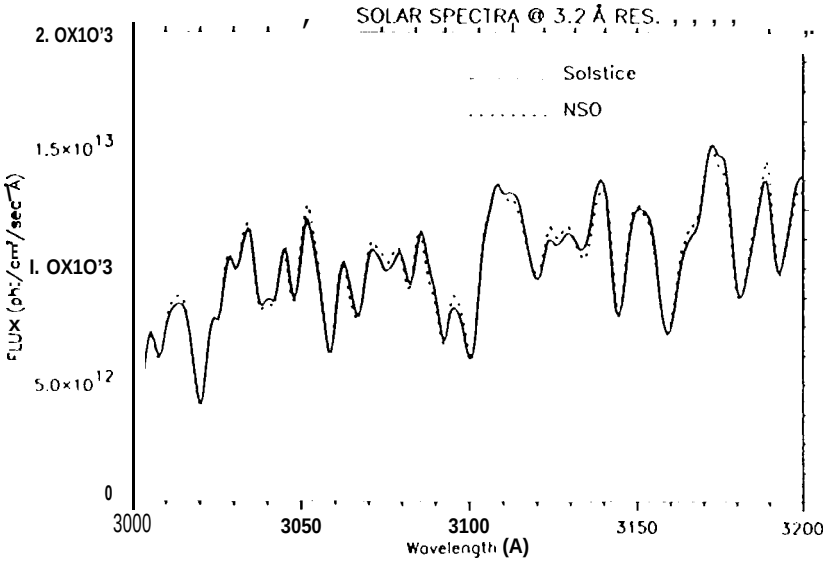

Fig. 2c

TABLE CAPTIONS

Table	Caption
Ia	Term values (units of cm^{-1}) for the F_1 and F_2 rotational levels of the $^2\Sigma$ state referenced to the $^2\Pi f_{1c}$ (N"= 1) level
1b	Term values (units of cm^{-1}) for the f_{1c}, f_{1d}, f_{2c}, f_{2d} rotational levels of the $^2\Pi$ state referenced to the $^2\Pi f_{1c}$ (N"= 1) level.
2	Calculated Einstein A coefficients for rotational transitions within the $A^2\Sigma \rightarrow X^2\Pi$ (0,0) band of OH; lifetime, $\tau_{0\,v}$, equal to 688ns.
3	Calculated 200, 240, 300K rotat ions] popul at ion partition function tabulated by transition from N" level (transitions are grouped according to starting N" states).
4	Calculated OH g-factor at 200, ?40, and 300K for all OH rotational lines to N"=15 and integrated solar flux (photon/cm^2/sec/Å) used for each line. OH (0,0) band oscillater strength equal to 1.04×10^{-3}.
5	The ten strongest OH lines (largest line. g-factors) at. 240K. The list includes emission line transition designat ion and wave length, absorption 1 ine transitions and wave le ngths pumping the $A^2\Sigma$ emit.t.ing state, solar flux, Einstein coefficients, relative population, line strengths at each absorption line, and the resulting emission line g-factor (phot,ons/see).
6	Percent changes in the OH g-factor for the ten strongest lines at 240K caused by $\pm$ 0.1cm^{-1} Shi fts in the solar spectrum, Absorption lines which populate the emitting state (see Table 5) and the solar flux values in units of photons /cm2/sec/Å are given before and after the spectral shifts. The percent. change in the emission rate factor rel ative to the unshifted spectrum is listed for the emission lines.

TABLE 1a

N	f1	f2
0	32440.540	0.000
1	32474.579	32474.225
2	32542.488	32541.901
3	32644.171	32643.350
4	32779.479	32778.425
5	32948.214	32946.930
6	33150.133	33148.621
7	33384.942	33383.204
8	33652.298	33650.339
9	33951.817	33949.636
10	34283.059	34280.663
11	34645.545	34642.936
12	35038.751	35035.932
13	35462.102	35459.080
14	35914.985	35911.765
15	36396.743	36393.329

TABLE 1b

f1c(N* 1) = 0.000

N*	f1c	f1d	f2c	f2d
1	0.000	0.056	126.449	126.291
2	83.719	83.920	187.751	187.491
3	201.922	202.370	289.041	288.769
4	355.105	355.900	429.458	429.275
5	543.575	544.809	608.188	608.194
6	767.458	769.216	824.525	824.813
7	1026.730	1029.092	1077.854	1078.509
8	1321.252	1324.291	1367.617	1368.720
9	1650.790	1654.577	1693.290	1694.914
10	2015.036	2019.633	2054.353	2056.568
11	2413.613	2419.081	2450.279	2453.149
12	2846.089	2852.485	2880.525	2884.110
13	3311.982	3319.355	3344.522	3348.880
14	3810.759	3819.156	3841.676	3846.859
15	4341.846	4351.310	4371.365	4377.419

TABLE 2

Einstein A Coefficients ($\times 10^{-5}$), Lifetime=688ns

N"	P1	P2	Q1	Q2	R1	R2	OP12	PQ12	QP21	QR12	RQ21	SR21
1	8.6110	0.0000	4.1080	4.8260	0.8091	1.2120	0.0000	4.8100	5.7350	:.2040	1.8030	0.2305
2	5.7770	3.9700	5.1500	4.9740	1.4040	1.7110	1.1140	2.6670	2.6460	1.1250	".5570	0.2756
3	4.9550	3.848o	5.7000	5.4660	1.8310	2.0580	0.7357	I.8750	1.6180	O.922I	:.2280	0.2569
4	4.5630	3.8350	6.0230	5.843o	2.1370	2.3130	0.5175	:.3770	1.1020	0.7315	0.9577	0.2221
5	4.3190	3.8190	6.2160	6.0950	2.3520	2.4980	0.3767	1.0370	0.7s?60	0.5777	0.7527	0.1873
5	4.1410	3.785o	6.3:70	6.2520	2.5020	2.6290	0.2819	0.7991	0.5995	0.4589	0.5989	0.1569
7	3.9970	3.7370	5.3570	6.3320	2.6040	2.7170	0.2162	0.6276	0.4656	0.3682	0.4835	0.1319
8	3.868o	3.6800	6.3470	6.3600	2.6710	2.773o	0.1695	0.5020	0.3702	0.2991	0.3953	[illegible]
9	3.7450	3.6110	6.3040	6.3420	2.7070	2.8060	0.1352	0.4077	0.2999	0.2458	0.3274	0.0949
' o	3.6280	3.532o	6.2360	6.2930	2.722o	2.8160	0.1096	0.3359	0.2469	0.2041	0.2742	0.0814
1 1	3.5160	3.4490	6.1390	6.2200	2.7780	2.81oo	0.0900	0.2801	0.2050	0.1711	0.2317	0.0704
12	3.4020	3.362o	6.0250	6.1200	2.6970	2.7910	0.0749	0.2359	0.1737	0.1447	0.1975	0.0611
13	3.2890	3.2670	5.8880	6.0020	2.6640	2.7560	0.0629	0.2005	0.1478	0.1232	0.1695	0.0534
14	3.1720	3.1700	5.7390	5.8640	2.6190	2.7110	0.0533	0.1715	0.1267	0.1055	0.1464	0.0469
' 5	3.0590	3.0670	5.5770	5.7120	2.5610	2.5580	0.0455	0.1478	0.1095	0.091[illegible]	0.1271	0.0413

TABLE 3

N"	['1, R1, RQ21	P2, R2, PQ12	Q1, QP21, SR21	Q2, OP12, QR12
1 emperature = 200.0 K		Q, = 2G,7101?O		
1	1.498[--01	3.015[-07	1.497[-01	3.018[-02
?	1.230[-01	3.880[-02	1.228[-01	3887[-02
3	7.00-/[-02	2.808[-02	6.985[-02	2.814[-02
4	2.910[-02	1.364[-02	2.893[-02	1 365[-02
5	9.000[-03	4."/12[-03	8.9?0[-03	4711[-03
6	2.097 ["-03	1.19?[-03	2.071 [-03	1.190 [.-03
7	3.712[-04	2.249[-04	3.650[-04	2.?38[-04
8	5.01 9E-0S	3.196[-0s	4.911[-0s	3.171[-05
9	5.?10[--06	1454[-06	5.070[-06	3.414 ["-06
10	4.171 [-07	2.857[-07	4.035 [-07	2.812[-07
11	2.587E-08	1.821 L-08	2.487 ['-08	1.784 E-08
12	1.248E-09	8.9 W["-10	1.192E-09	8.765E-10
13	4.709[.-11	3.460[11	4.465[-11	3.353[-11
14	1.395 E-12'	1.042[-12	1.313[. 12	1.004[-12
15	3.261E-14	2.472E-14	3.046 ["-14	2.367[-14
sum	0.383454	0.1 16829	0.382712	0.117005
1 emperature = 240.0 K"		Q, = 32.239399		
1	1.2'41 [-01	2.907[-o?	1.240[-01	2,910 ['-02
2	1.127[-01	4.026[-02	1.125[-01	4.032[-02
3	7.396E-02	3.290E-02	7.376E-02	3.296E-02
4	3.690E-02	1.891 E-O?	3.673E-02	1.893E-02
5	1.431 E-02	8.094E-03	1.420E-02	8.093E-03
6	4.361 E-03	2.655[-03	4.316E-03	2.651[-03
7	1.053[-03	6.784[-04	1.039E-03	6.757E-04
8	2.027E-04	1.365[-04	1.991 E-04	1.356[-04
9	3.124[-05	2.179[-05	3.054E-05	2.158E-05
10	3.870E-06	2.780E-06	3.765E-06	2.743[-06
11	3.871 E-07	2.848E-07	3.746E-07	2.800[-07
12	3.138E-08	2.356E-08	3.020E-08	2.306E-08
13	2.069E-09	1.581 E-09	1.980E-09	1.540E-09
14	1.115E-10	8.644E-11	1. O6OE-10	8.379E-11
15	4.926E-12	3.869E-12	4.654E-12	3.731 E-12
Sum	0.367560	0.132722	0.366839	0.132878
Temperature = 300.0 K		Q_r = 40.748164		
1	9.816E-02	2.676E-02	9.814E-02	2.678E-02
2	9.8 55E-02	3.989[-02	9.846E-02	3.994[-02
3	7.454E-02	3.681 E-O?	7.438E-02	3.686E-02
4	4.469E-02	2.503[-02	4.452E-02	2.505E-02
5	2.172 E-02	1.328E-02	2.159E-02	1.328E-02
6	8.660E-03	5.646E-03	8.587E-03	5.638 E-03
7	2.854E-03	1.954E-03	2.822E-03	1.948E-03
8	7.820E-04	5.565E-04	7.706E-04	5.536E-04
9	1.789E-04	1.31 3E-04	1.757E-04	1.303E-04
1 0"	3.430E-05	2.582E-05	3.355E-05	2.555E-05
11	5.532E-06	4.253E-06	5.389E-06	4.195E-06
12	7.531 E-07	5.894[-07	7.304E-07	5.793E-07
13	8.683E-08	6.898[-08	8.381 E-08	6.755E-08
14	8.506E-09	6.845 [--09	8.171 E-09	6.677[-09
15	7.1 OGE-10	5.782[-10	6.790[-10	5.617 E-10
Sum	0.350191	0.150098	0.349492	0.150219

TABLE 4

$f_{0,0} = 1.04 \times 10^{-3}$

Transition	JJ	J	Wavelength(Å)	Solar Flux (pht/cm²/sec/Å)	g-factor (pht/s) 200K	240K	300K
OP12(15)	14.5	13.5	3216.0896	1.9218E+13	6.02E-16	1.60E-14	4.20E-13
OP12(14)	13.5	12.5	3205.0352	1.9102E+13	1.32E-14	2.13E-13	3.46E-12
OP12(13)	12.5	11.5	3194.3052	1.7435E+13	2.32E-13	2.34E-12	2.36E-11
OP12(12)	11.5	10.5	3183.8992	1.0542E+13	4.20E-12	2.72E-11	1.75E-10
OP12(11)	10.5	9.5	3173.8193	1.9708E+13	4.35E-11	1.94E-10	8.59E-10
P2(15)	14.5	13.5	3169.6196	5.1535E+12	2.31E-15	9.69E-14	4.20E-12
PQ12(15)	14.5	14.5	3169.2961	1.4928E+13	5.36E-17	2.56E-15	1.24E-13
P1(15)	15.5	14.5	3166.3330	4.7851E+12	1.11E-15	5.30E-14	2.56E-12
OP12(10)	9.5	8.5	3164.0686	5.7139E+12	4.54E-10	1.43E-09	4.48E-09
P2(14)	13.5	12.5	3161.8999	3.8034E+12	5.59E-14	1.36E-12	3.41E-11
PQ12(14)	13.5	13.5	3161.5977	1.2790E+13	2.27E-15	6.02E-14	1.58E-12
P1(14)	14.5	13.5	3158.5093	4.2996E+12	4.20E-14	1.11E-12	2.93E-11
OP12(9)	8.5	7.5	3154.6533	6.5143E+12	3.38E-09	7.88E-09	1.82E-08
P2(13)	12.5	11.5	3154.5156	2.3927E+12	2.09E-12	2.41E-11	2.94E-10
PQ12(13)	12.5	12.5	3154.2354	3.2299E+12	4.95E-14	8.02E-13	1.30E-11
P1(13)	13.5	12.5	3151.0000	4.5045E+12	8.12E-13	1.31E-11	2.13E-10
P2(12)	11.5	10.5	3147.4639	4.3212E+12	3.78E-11	2.82E-10	2.21E-09
PQ12(12)	11.5	11.5	3147.2053	3.1786E+12	8.70E-13	8.78E-12	8.84E-11
OP12(8)	7.5	6.5	3145.5820	1.5016E+13	1.83E-08	3.28E-08	5.77E-08
P1(12)	12.5	11.5	3143.7971	2.1580E+12	1.25E-11	1.27E-10	1.28E-09
P2(11)	10.5	9.5	3140.7424	3.6534E+12	2.32E-10	1.39E-09	8.38E-09
PQ12(11)	10.5	10.5	3140.5061	1.3345E+13	1.58E-11	1.03E-10	6.66E-10
P1(11)	11.5	10.5	3136.8926	3.6367E+12	1.98E-10	1.29E-09	8.36E-09
OP12(7)	6.5	5.5	3136.8672	6.4637E+12	4.45E-08	7.10E-08	1.10E-07
P2(10)	9.5	8.5	3134.3516	3.1869E+12	3.17E-09	1.18E-08	4.55E-08
PQ12(10)	9.5	9.5	3134.1372	8.9540E+11	1.62E-10	7.25E-10	3.20E-09
P1(10)	10.5	9.5	3130.2788	1.4203E+12	1.75E-09	7.83E-09	3.46E-08
OP12(6)	5.5	4.5	3128.5266	8.4130E+12	3.17E-07	3.89E-07	4.65E-07
P2(9)	8.5	7.5	3128.2935	3.7101E+12	1.55E-08	4.57E-08	1.34E-07
PQ12(9)	8.5	8.5	3128.1016	1.1293E+13	1.69E-09	5.32E-09	1.67E-08
P1(9)	9.5	8.5	3123.9470	3.6794E+12	1.55E-08	4.89E-08	1.53E-07
P2(8)	7.5	6.5	3122.5732	2.9468E+12	1.62E-07	3.22E-07	6.45E-07
Q2(15)	14.5	14.5	3122.5417	2.9970E+12	2.05E-16	1.27E-14	8.44E-13
PQ12(8)	7.5	7.5	3122.4038	9.5652E+12	1.25E-08	2.93E-08	6.76E-08
QR12(15)	14.5	15.5	3122.2087	5.3362E+12	1.72E-18	1.43E-16	1.16E-14
OP12(5)	4.5	3.5	3120.5857	1.0127E+13	9.84E-07	1.02E-06	1.03E-06
QP21(15)	15.5	14.5	3119.9973	1.2585E+13	3.93E-18	2.43E-16	1.62E-14
Q1(15)	15.5	15.5	3119.6648	3.0993E+12	1.05E-16	8.73E-15	7.11E-13
P1(8)	8.5	7.5	3117.8884	3.0584E+12	9.67E-08	2.26E-07	5.21E-07
Q2(14)	13.5	13.5	3117.7703	3.3188E+12	4.41E-15	1.85E-13	8.03E-12
QR12(14)	13.5	14.5	3117.4570	1.1551E+13	3.83E-17	1.83E-15	8.84E-14
P2(7)	6.5	5.5	3117.2004	3.8207E+12	6.08E-07	9.50E-07	1.48E-06
PQ12(7)	6.5	6.5	3117.0535	9.2941E+12	6.79E-08	1.21E-07	2.14E-07
QP21(14)	14.5	13.5	3115.0789	9.5990E+12	9.54E-17	4.00E-15	1.73E-13
Q1(14)	14.5	14.5	3114.7664	3.4057E+12	2.08E-15	9.93E-14	4.80E-12
Q2(13)	12.5	12.5	3113.3723	2.9589E+12	1.06E-13	2.58E-12	6.45E-11
OP12(4)	3.5	2.5	3113.0801	1.1950E+13	1.89E-06	1.80E-06	1.67E-06
QR12(13)	12.5	13.5	3113.0791	1.1950E+13	1.63E-15	4.32E-14	1.14E-12
P2(6)	5.5	4.5	3112.1892	3.6889E+12	1.44E-06	2.07E-06	2.92E-06
P1(7)	7.5	6.5	3112.0925	1.9362E+12	4.33E-07	7.73E-07	1.36E-06
PQ12(6)	5.5	5.5	3112.0647	1.7740E+12	1.64E-07	2.63E-07	4.08E-07
QP21(13)	13.5	12.5	3110.5120	1.1166E+13	2.61E-15	6.35E-14	1.59E-12
Q1(13)	13.5	13.5	3110.2195	2.4901E+12	7.80E-14	2.07E-12	5.44E-11
Q2(12)	11.5	11.5	3109.3416	2.7861E+12	3.92E-12	4.52E-11	5.50E-10

TABLE 4 (cont.)

$f_{0,0} = 1,()< \times 10^{-3}$

Transition	JJ	J	Wavelength(Å)	Solar Flux (pht/cm²/sec/Å)	g-factor (pht/s) ?oOK	240K	300K
QR12(12)	11.5	12.5	31090691	5.3668E+12	3.57E-14	5.79E-13	9.39E-12
P2(5)	4.5	3.5	3107.5618	3.7401E+12	5.36E-06	6.31E-06	7.23E-06
PQ12(5)	4.5	4.5	3107.4GOO	7.2034E+12	1.17E-06	1.43E-06	1.71E-06
P1(6)	6.5	5.5	3106.5459	2.6544E+12	8.5?[-07	1.36E-06	2.11E-06
QP21(12)	12.5	11.5	3106.2859	8.5571E+2	I.II[-13	1.28E-l?	1.56E-11
OP12(3)	2.5	1.5	31 OG. O581	6.5341[+2	2.38E-06	2.19E-06	1.95E-06
Q1(12)	12.5	1?.5	31 OG. O142	3.1424E+?	1.49E-12	241[-11	3.91E-10
Q2(11)	10.5	10.5	3105.6743	2.9079E+2	7.00E-11	5.23E"-10	4.09E-09
QR12(11)	10.5	11.5	3105,4?26	4.9082E+2	6.31E-13	6.37E-12	6.41E-11
P2(4)	3.5	2.5	3103.3503	4.6882E+?	1.27E-05	1.26E-05	1.21E-05
PQ12(4)	3.5	3.5	3103.2'71?	6.5004E+2	3.60E-06	3.74E-06	3.78E-06
QP21(11)	11.5	10.5	3102.3909	3.7112E+2	2.3?[-12	1.73E--11	1.35E-lo
Q2(10)	9.5	9.5	310?.3677	2.0681E+2	4.23[.-10	2.53E-09	1.53E-08
Q1(11)	11.5	11.5	3102.1396	2.8176E+?	2.26E-11	2.?9["-10	?.30[-09
QR12(10)	9.5	10.5	3102,1370	2.9722E+?	1.15E-11	7.49E--1 1	4.85E-10
P1(5)	5.5	4.5	3101.? 312	3.3627E+2	4.86E-06	5.96E-06	7.13E-06
P2(3)	2.5	1.5	3099.6006	4.7668E+12	9.1 OE-O6	8.79E-06	8.20E-06
OP12(2)	1.5	0.5	3099.58?5	4.6742E+12	3.02E-06	2.63E-06	2.21E-06
PQ1?(3)	2.5	2.5	3099.544?	5.4760E+12	6.83E-06	6.53E-06	6.03E-06
Q2(9)	8.5	8.5	3099.4?16	2.8918E+12	5.69E-09	2.12E-08	8.17E-08
QR12(9)	8.5	9.5	3099.21??	6.6295E+12	1.19E-10	5.3 OE-10	2.35E-09
QP21(10)	10.5	9.5	3098.8159	5.5342E+12	1.66E-11	9.93E-11	6.00E-lo
Q1(10)	10.5	10.5	3098.5857	2.7953E+12	3.52E-10	2.29E-09	1.48E-08
Q2(8)	7.5	7.5	3096.8391	1.7925E+12	2.74E-08	8.04E-08	2.37E-07
QR12(8)	7.5	8.5	3096.6511	4.8084E+12	1.24E-09	3.90E-09	1.? '2[-08
P2(2)	1.5	0.5	3096.3/'33	5.1043E+12	9.12E-06	8.24E-06	7.17E-06
PQ1 2(2)	1.5	1.5	3096.3396	4.5560E+12	8.63E-06	7.96E-06	7.05E-06
PI (4)	4.5	3.5	3096.1250	2.9154E+12	1.19E-05	1.24E-05	1.25E-05
QP21 (9)	9.5	8.5	3095.5503	1.3117E+13	2.69E-10	1.00E-09	3.87E-09
Q1(9)	9.5	9.5	3095.3413	2.8586E+12	3.05E-09	1.36E-08	6.01E-08
Q2(7)	6.5	6.5	3094.6270	2.9228E+12	2.79E-07	5.54E-07	1.11E-06
QR12(7)	6.5	7.5	3094.4604	9.8042E+12	9.20E-09	2.15E-08	4.96E-08
PQ12(1)	0.5	0.5	3093.7?71	6.0770E+2	1.30E-05	1.14E-05	9.52E-06
Q2(6)	5.5	5.5	3092.7971	1.2518E+2	1.02E-06	1.59E-06	2.48E-06
QR12(6)	5.5	6.5	3092.6523	2.1870E+2	4.97E-08	8.88E-08	1.56E-07
QP21(8)	8.5	7.5	3092.5828	3.9033E+2	1.59E-09	4.68E-09	1.38E-08
Q1(8)	8.5	8.5	3092.3953	2.6367E+2	2.63E-08	8.28E-08	2.60E-07
Q2(5)	4.5	4.5	3091.3694	2.8486E+2	2.32E-06	3.34E-06	4.71E-06
QR12(5)	4.5	5.5	3091.2466	5.3192E+2	1.19E-07	1.90E-07	2.95E-07
P1(3)	3.5	2.5	3091.1943	2.9768E+2	1.81E-05	1.72E-05	1.59E-05
Q2(1)	0.5	0.5	3090.4902	6.4004E+2	1.11E-05	1.00E-05	8.71E-06
QR12(1)	0.5	1.5	3090.4565	6.9536E+2	3.89E-06	3.59E-06	3.18E-06
Q2(4)	3.5	3.5	3090.3740	3.1574E+2	8.20E-06	9.65E-06	1.11E-05
QR12(4)	3.5	4.5	3090.2734	6.4996E+2	8.24E-07	1.01E-06	1.21E-06
QP21(7)	7.5	6.5	3089.9001	4.7265E+2	2.05E-08	4.07E-08	8.16E-08
Q2(2)	1.5	1.5	3089.8716	2.7516E+2	1.18E-05	1.14E-05	1.06E-05
Q2(3)	2.5	2.5	3089.855'2	2.7573E+2	1.81E-05	1.79E-05	1.73E-05
QR12(2)	1.5	2.5	3089.8157	4.4721E+2	4.1 OE-OG	3.92E-06	3.62E-06
QR12(3)	2.5	3.5	3089.7771	3.8328E+?	?.41E-06	2.50E-06	2.53E-06
Q1(7)	7.5	7.5	3089.7341	2.5701E+12	1.59E-07	3.71E-07	8.57E-07
QP21 (6)	6.5	5.5	3087.4863	7.6437E+12	9.75E-08	1.52E-07	2.38E-07
Q1(6)	6.5	6.5	3087.34?3	2.6544E+12	6.84E-07	1.22E-06	2.15E-06
P1 (2)	2.5	1.5	3086.3945	3.8533E+12	1.87E-05	1.72E-05	1.53E-05
QP21(5)	5.5	4.5	3085.3218	6.3380E+12	3.04E-07	4.36E-07	6.15E-07

TABLE 4 (cont.)

$f_{0,0}$ = 1. O4X1O3

Transition	J J	J	Wavelength(Å)	Solar Flux (pht/cm²/sec/Å)	g-factor (pht/s) 200K	240K	300K
Q1(5)	5.5	5.5	3085.1 995	2.7909E+ 1?	1.28E-06	2.04["-06	3.17E-06
R2(1)	0.5	1.5	3084.0527	8.9906E+1 '?	2.87E-06	2.77E-06	2.58E-06
QP21(4)	4.5	3.5	3083.3799	7.7470E+12	1.55E-06	1.82E-06	2.08E-06
Q1(4)	4.5	4.5	3083. ?798	2.8717E+12	6.78[-06	8.31E-06	9.94E-06
P1(1)	1.5	0.5	3081.6677	3.5450[+ 12	2.33E-05	2.03E-05	1.70E-05
(2['? 1(3)	3.5	2.5	3081.6260	4.9-/09[+12	5.35E-06	5.31E-06	5.12E-06
Q1(3)	3.5	3.5	3081.5479	?.9581[+ 12	1.49E-05	1.55E-05	1.56E-05
R2(2)	1.5	2.5	3080.2378	7.8644[+12	5.66E-06	5.61E-06	5.41E-06
QP21(2)	2.5	1.5	3080.0117	3.4542E + 1'2	6.26E-06	6.04E-06	5.64E-06
Q1(2)	2.5	2.5	3079.9561	3.1738E+12	1.88E-05	1.79E-05	1.66E-05
QP21(1)	1.5	0.5	3078.4763	3.3731E+12	1.32E-05	1.19E-05	1.04 E-05
Q1(1)	1.5	1.5	3078.4429	1.6130E+12	1.33E-05	1.23E-05	1.09E-05
R2(3)	2.5	3.5	3077.0347	6.0449E+12	2.89E-06	3.40E-06	3.89E-06
R2(4)	3.5	4.5	3074.3765	4.6141E+12	8.82E-07	1.27E-06	1.79[-06
R2(I 5)	14.5	15.5	3073.0310	2.4444[+12	1.58E-18	1.74E-16	2.04E-14
R2(5)	4.5	5.5	3072.2073	3.7399[+12	4.06E-07	6.35E-07	9.91E-07
RQ21(1)	1.5	1.5	3072.0686	1.9467E+12	4.26E-06	4.12E-06	3.84E-06
R1(1)	1.5	?.5	3072.0132	5.2488E+12	2.95E-06	2.82E-06	2.60E-06
R2(14)	13.5	14.5	3071.1482	3.6368E+12	9.72E-17	6.01E-15	4.01E-13
R2(6)	5.5	6.5	3070.4856	4.1097F 41?	1.16E-07	2.30E-07	4.61E-07
RQ21(2)	2.5	2.5	3070.3955	8.2180E+12	5.15E-06	5.11E-06	4.92E-06
R1(2)	2.5	3.5	3070.3181	5.8408[+ 12	3.67E-06	3.81 E-06	3.85E-06
RQ21(15)	15.5	15.5	3070.2451	3.3753E+12	7.55E-20	8.32E-18	9.75E-16
R1(15)	15.5	16.5	3069.9053	4.8446E+12	1.49E-18	2.25E-16	3.24E-14
R2(13)	12.5	13.5	3069.6780	3.7685E+12	2.07E-15	8.71 E-14	3.77E-12
R2(7)	6.5	7.5	3069.1841	3.8506E+12	1.17E-08	3.44E-08	1.01E-07
RQ21(3)	3.5	3.5	3068.8054	6.7783E+ 2	1.72E-06	2.03E-06	2.32E-06
R1(3)	3.5	4.5	3068.7061	3.6546E+ 2	2.06E-06	2.53E-06	3.02E-06
R2(12)	11.5	12.5	3068.6121	3.3771E+ 2	4.93E-14	1.20E-12	3.00 E-I 1
R2(8)	7.5	8.5	3068.2859	3.4797E+ 2	2.49E-09	9.27E-09	3.57E-08
RQ21(14)	14.5	14.5	3068.2339	6. O41OE-I 2	5.25E-18	3.24E-16	2.16E-14
R2(11)	10.5	11.5	3067.9436	1.9960E+ 2	1.80E-12	2.07E-11	2.52E-10
R1(14)	14.5	15.5	3067.9124	3.5482E+ 2	4.95E-17	4.1 OE-15	3.34E-13
R2(9)	8.5	9.5	3067.7817	3.4440E+ 2	1.88E-10	1.13E-09	6.82E-09
R2(10)	9.5	10.5	3067.6677	3.1974E+ 2	3.17E-11	2.37E-10	1.85E-09
RQ21(4)	4.5	4.5	3067.3625	2.8525E+ 2	3.65E-07	5.24E-07	7.39E-07
R1(4)	4.5	5.5	3067.2417	5.3621E+ 1	4.40E-07	7.02E-07	1.09[--06
RQ21(13)	13.5	13.5	3066.6138	1.1648E+ 3	1.28E-16	5.36E-15	2.32E-13
R1(13)	13.5	14.5	306 I3.31O8	2.0014E+12	9.67E-16	4.61E-14	2.23E-12
RQ21(5)	5.5	5.5	3066.1189	4.7003E+12	1.22E-07	1.91 E-07	2.99E-07
RI (5)	5.5	6.5	3065.9766	3.3906E+12	2.55E-07	4.55E-07	8.01E-07
RQ21(12)	12.5	12.5	3065.3718	1.0996E+13	3.49E-15	8.49E-14	2.12E-12
RQ21 (6)	6.5	6.5	3065.1128	3.5431E+12	2.64E-08	5.24E-08	1.05E-07
R1(12)	12.5	13.5	3065.0879	3.009 6E+12	3.57E-14	9.46E-13	2.49E-11
RI (6)	6.5	7.5	3064.9497	3.3193E+12	6.25E-08	1.46E-07	3.37E-07
RQ21(11)	11.5	11.5	3064.4951	1.0033E+13	1.49E-13	1.71 E-12	2.08E-11
RQ21(7)	7.5	7.5	3064.3740	2.989 6E+12	2.08E-09	6.11E-09	1.80E-08
R1(11)	11.5	12.5	30 64.2305	2.6871E+12	6.71E-13	1.09E-11	1.7 GE-10
R1(7)	7.5	8.5	3064.1899	3.1792E+12	1.08E-08	3.40E-08	1.06E-07
RQ21(10)	10.5	10.5	3063.9709	5.6277E+12	3.08E-12	2.30E-11	1.80E-10
RQ21(8)	8.5	8.5	3063.9255	2.5049E + 12	3.55E-10	1.32E.-O9	5.09 E-09
RQ21(9)	9.5	9.5	3063.7859	7.7451E+12	2.20E-11	1.32E-10	7.96E-10
R1(10)	10.5	11.5	3063.7261	2.5323E+12	1.00 E-1 1	1.01E-10	1.02E-09
R1(8)	8.5	9.5	3063.7?07	2.6688E+12	1.29E-09	5.76E-09	2.55E-08

TABLE 4 (cont.)

$f_{0,0}$ = 1.04 x 10^3

Transition	J J	J	Wavelength(Å)	Solar Flux (pht/cm²/sec/Å)	g-factor (pht/s) ?OOK	240K	300K
R1(9)	9.5	10.5	3063.5608	3.1689[+12	1.53E -10	9.93E -10	6.44E -09
SR21(1)	1.5	2.5	30(;2.5'259	1.2034[+13	7.62E -0-/	7.56[--07	7.29E -07
SR21(2)	2.5	3.5	3057 7290	2.8401E +12	3.87E -07	4.55E -07	5.21E -07
SR21(3)	3.5	4.5	3053.0544	2.4209E +12	9.80E -08	1 .41E -07	1.98E -07
SR21(4)	4.5	5.5	3048.5703	1.1091E +13	3.61 [-08	5.64E-08	8.81E -08
SR21(5)	5.5	6.5	3044.3301	1.3631E+13	8.26E -09	1.64E -08	3.28E -08
SR21(6)	6.5	7.5	3040.3740	2.9203E+12	6.75[. -10	1.98E-09	5.84E -09
SR21(7)	7.5	8.5	3036.7332	9.6358E+12	1.18E-10	4.41[-10	1.70E-09
SR21(8)	8.5	9.5	3033.4316	2.7465E+12	7.49E-12	4.48E -11	?.71['-10
SR21(9)	9.5	10.5	3030.4900	1.4996E+13	1.07E-12	7.98E-12	6.24E-11
SR?1(10)	10.5	11.5	30?-7.9?53	1.2760E+13	5.22E-14	6.01E-13	7.32E-12
SR21(11)	11.5	12.5	3025.7534	2,1300 [.4 12	1.24E-15	3.02E-14	7.56E -13
SR21(12)	12.5	13.5	30?3.9888	2.1571E+12	4.60 E-17	1.93[-15	8.36E -14
SR21(13)	13.5	14.5	3022.6450	7.2660E+12	1.91E-18	1.18E-16	7.89E-15
SR21(14)	14.5	15.5	3021.-/366	4.6434E+12	2.78E-20	3.07E-18	3.59["-16
SR21(15)	15.5	16.5	3021.2769	2.2247E+12	1.55E-22	2.37E-20	3.45[--18

The total (0,0) band g value of OH at T = 240.0 K is 3.42 x 10^{-4} photos/see.

TABLE 5

Emission Trans	Emission Wave(Å)	Absorption Trans.	Absorption Wave(A)	Solar Irradiance (pht/cm²/sec/Å)	Population (240K) (N/N₀)	Einstein A Coefficient (xl O')	Line Strength S(J,J″)	g(240 k) (pht/sec) (X1O')'
$P_1(1)$	3081.6677					(8.611)		2 03
		PI(1)	3081.6677	3.5450E+12	0.1241	8.661	2.3564	
		^{O}P12(2)	3099.58?5	4.6742E+12	0,0403	1.114	0.310?	
		^{P}Q12(1)	3093.7?71	6.0770[+12	0.0291	4.810	1.3333	
-(2_3(3)	3089.8552					(5.467)		1.79
		P.?(4)	3103.3503	4.6882E+12	0.0189	3.835	3.2347	
		Q2(3)	3089.8552	2.7573E+12	0.0329	5.467	4.5555	
		R2(2)	3080.2378	7.8644E+12	0.0403	1.711	1.4129	
		^{O}P21(3)	3081 6260	4.9709E+12	0.0737	1.618	1.3365	
		'0?1(2)	3070.3955	8.2180E+1?	0.1127	1.803	1.2730	
		^{S}R21(1)	3062.5259	1.2034E+13	0.1240	2.305	0.1870	
Q_1(2)	3079.9561					(5. 1 50)		1.79
		P1(3)	3091.1943	2.9768E+1?	0.0740	4.955	4.1304	
		Q1(2)	3079.9561	3.1738 E+1?	0.1125	5.150	4.2511	
		R1(1)	3072.0132	5.2488E+12	0.1241	0.809	0.6627	
		^{P}Q12(3)	3099.5442	5.4760E+12	0.0329	1.875	1.5773	
		^{O}P12(4)	3113.0801	1.1950E+13	0.0189	0.517	0.4406	
		^{O}R12(2)	3089.8157	4.4721E+12	0.0403	1.125	0.9372	
I',(3)	3091.1943					(4.955)		1.72
		P1(3)	3091.1943	2.9768E+12	0.0740	4.955	4.1304	
		Q 1 (2)	3079.9561	3.1738E+12	0.1125	5.150	4.2511	
		R1(1)	3072.0132	5.2488E+1?	0.1241	0.809	0.6627	
		^{P}Q12(3)	3099.5442	5.4760E+1?	0.0329	1.875	1.5773	
		^{O}P12(4)	3113.0801	1.1950E+13	0.0189	0.517	0.4406	
		^{O}R12(2)	3089.8157	4.4721E+12	0.0403	1.125	0.9372	
p_1(2)	3086.3945					(5.777)		1.72
		Pi(2)	3086.3945	3.8533E+12	0.1127	5.777	3.1863	
		Q1(1)	3078.4429	1.6130 E+12	0.1240	4.108	2.2482	
		^{O}P12(3)	3106.0581	6.5341 E+12	0.0329	0.736	0.4136	
		^{P}Q12(2)	3096.3396	4.5560E+12	0.0403	2.667	1.4851	
		^{O}R12(1)	3090.4565	6.9536E+12	0.1240	1.204	0.6666	
Q_1(3)	3081.5479					(5.700)		1.55
		Pi(4)	3096.1250	2.9154E+12	0.0369	4.563	5.1219	
		Q1(3)	3081.5479	2.9581E+12	0.0738	5.700	6.3144	
		R 1 (2)	3070.3181	5.8408E+12	0.1127	1.404	1.5404	
		^{O}P12(5)	3120.5857	1.0127 E+13	0.0081	3.767	0.4329	
		^{P}Q12(4)	3103.2712	6.5004E+12	0.0189	1.377	1.5584	
		^{O}R12(3)	3089.7771	3.8328E+12	0.0330	0.922	1.0308	
P_2(4)	3103.3503					(3.853)		1.26
		P2(4)	3103.3503	4.6882 E-r 12	0.0189	3.835	3.2348	
		Q2(3)	3089.8552	2.7573E+12	0.0329	5.466	4.5555	
		R2(2)	3080.2378	7.8644E+12	0.0403	1.711	1.4129	
		^{O}P21(3)	3081.6260	4.9709E+12	0.0737	1.618	1.3365	
		^{R}Q21(2)	3070.3955	8.2180E+12	0.11'27	1.557	1.2730	
		^{S}R21(1)	3062.5259	1.2034E+13	0.1240	0.231	0.1871	

TABLE 5 [cont.)

Emission 1rans	wave(A)	Absorption 1rans.	Wave(A)	Solar Irradiance (pht/cm²/sec/Å)	Population (240K) (N/N_0)	Einstein A Coefficient (xl O')	Line Strength S(J,J")	(240 k) iptlt/sot) (xl o ⁵)
$P_1(4)$	3096 1250					(4.563)		1.?4
		P1(4)	3096.1250	?.9154[+ 1?	0.0369	4.563	5.1219	
		Q1(3)	3081.5479	2.9581E+1?	0.0738	5.700	6.3144	
		R1(2)	3070.3181	5.8408[+12	0.1127	1.404	1.5404	
		^{o}P12(5)	31?0.585-/	1.0127E+13	0.0081	3.767	0.4329	
		^{P}Q12(4)	3103.2712	6.5004[i 12	0.0189	1.377	1.5584	
		^{o}R12(3)	3089.7771	3.8328[+12	0.0330	0.92?	1.0308	
Q,(I)	3078.44?9					v o l j - -		1.?3
		P1(2)	3086.3945	3.8533E+12	0.1127	5.777	3.1863	
		Q1(1)	3078.4429	1.6130E+12	0.1240	4.108	2.2482	
		^{o}P12(3)	31 OG.O581	6.5341E+12	0.03?9	0.736	0.4136	
		^{P}Q1 2(2)	3096.3396	4.5560E+12	0.0403	2.667	1.4851	
		^{o}R1 2(1)	3090.4565	6.9536E+12	0.1240	1.204	0.6666	
$^{o}P_{21}$ (1)	3078.4763					(m 3 q - -		1.19
		P2 (2)	309 6.3733	5.1043 E+1?	0.0403	3.970	1.1019	
		Q2 (1)	3090.4902	6.4004E+12	0.0291	4.826	1.3333	
		^{o}P21(1)	3078.4763	3.3731E+1?	0.1240	5.735	1.5646	

TABLE 6

Transition	Wavelength(Å)	Solar Flux (pht/cm²/s/Å)	g (pills)	Solar Flux (-0.1 cm⁻¹)	Δg (%)	Solar Flux (+0.1 cm⁻¹)	Δg (%)
0['1?(5)	31?0.5857	1.0127E+13		1.0437E+13		1.0486E+13	
OP12(4)	311:3.0801	1.1950E+13		1.2712E+13		1.2126E+13	
OP12(3)	3106.0581	6.5341E+12		4.9889E+12		9.3160E+12	
P?(4)	3103 3503	4.6882E+12	1.26E-05	4.8008E+12	0.79	5.5533E+12	8.73
PQ12(4)	3103.2712	6.5004E+12		7.1931E+12		6.4172E+12	
01'1?(2)	3099.5825	4.6742E+12		4.9765E+12		4.5625E+12	
PQ12(3)	3099.5442	5.4760E+12		6.0209E+12		5.3335E+12	
P?(2)	3096.3733	5.1043E+12		4.9443E+12		5.1248E+12	
PQ12(2)	3096.3396	4.5560E+12		4.4036E+12		4.7308E+12	
PI(4)	3096.12s0	2.9154E+12	1.24E-05	3.1019E+12	3.23	2.9646E+12	8.87
PQ12(1)	3093.7271	6.0770E+12		6.0806E+12		6.8048E+12	
P1(3)	3091.1943	2.9768E+12	1.72E-05	3.0823E+12	12.21	3.0788E+12	-5.81
Q2(1)	3090.4902'	6.4004E+12		5.8354E+12		7.2155E+12	
QR12(1)	3090.4565	6.9536E+12		7.9337E+12		6.2234E+12	
Q2(3)	3089.8552	2.7573E+12	1.79E-05	3.0437E+12	0.56	2.6770E+12	8.94
QR12(2)	3089.8157	4.4721E+12		4.8335E+12		3.9286E+12	
QR12(3)	3089.7771	3.8328E+12		3.1464E+12		4.3018E+12	
PI(2)	3086.3945	3.8533E+12	1.72E-05	4.5489E+12	8.72	4.3463E+12	9.88
PI(I)	3081.6677	3.5450E+12	2.03E-05	3.7472E+12	3.94	3.5130E+12	2.96
QP21(3)	3081.6260	4.9709E+12		5.4239E+1?		4.5581E+12	
Q1(3)	3081.5479	2.9581E+12	1.55E-05	3.2488E+12	3.23	3.0846E+12	9.03
m?(?)	3080.2378	7.8644E+12		7.7701E+12		9.3421E+12	
Q1(2)	3079.9561	3.1738E+12	1.79E-05	3.6037E+12	11.73	2.8621E+12	-6.15
QP21(1)	3078.4763	3.3731E+12	1.19E-05	2.8739E+12	-12.61	4.0278E+12	14.29
Q1(1)	3078.4429	1.6130E+12	1.23E-05	1.5945E+12	8.13	1.8792E+12	9.76
R1(1)	3072.0132	5.2488E+12		5.5399E+12		4.5737E+12	
RQ21(2)	3070.3955	8.2180E+12		7.9780E+12		8.9816E+12	
R1(2)	3070.3181	5.8408E+12		5.4357E+12		6.9118E+12	
SR21(1)	3062.5259	1.2034E+13		1.1465E+13		1.3204E+13	